

● *Original Contribution*

## QUANTITATIVE CHARACTERIZATION OF VISCOELASTIC PROPERTIES OF HUMAN PROSTATE CORRELATED WITH HISTOLOGY

MAN ZHANG,\* PRIYA NIGWEKAR,† BENJAMIN CASTANEDA,‡ KENNETH HOYT,‡  
JEAN V. JOSEPH,† ANTHONY DI SANT'AGNESE,† EDWARD M. MESSING,† JOHN G. STRANG,†  
DEBORAH J. RUBENS,† and KEVIN J. PARKER\*,‡

\*Department of Biomedical Engineering, University of Rochester; †University of Rochester Medical Center; and  
‡Department of Electrical and Computer Engineering, University of Rochester, Rochester, NY

(Received 6 June 2007, revised 21 November 2007, in final form 30 November 2007)

**Abstract**—Quantification of mechanical properties of human prostate tissue is important for developing sonoelastography for prostate cancer detection. In this study, we characterized the frequency-dependent complex Young's modulus of normal and cancerous prostate tissues *in vitro* by using stress relaxation testing and viscoelastic tissue modeling methods. After radical prostatectomy, small cylindrical tissue samples were acquired in the posterior region of each prostate. A total of 17 samples from eight human prostates were obtained and tested. Stress relaxation tests on prostate samples produced repeatable results that fit a viscoelastic Kelvin-Voigt fractional derivative (KVFD) model ( $r^2 > 0.97$ ). For normal ( $n = 8$ ) and cancerous ( $n = 9$ ) prostate samples, the average magnitudes of the complex Young's moduli ( $E^*$ ) were  $15.9 \pm 5.9$  kPa and  $40.4 \pm 15.7$  kPa at 150 Hz, respectively, giving an elastic contrast of 2.6:1. Nine two-sample *t*-tests indicated that there are significant differences between stiffness of normal and cancerous prostate tissues in the same gland ( $p < 0.01$ ). This study contributes to the current limited knowledge on the viscoelastic properties of the human prostate, and the inherent elastic contrast produced by cancer. (E-mail: [mazhang@seas.rochester.edu](mailto:mazhang@seas.rochester.edu)) © 2008 World Federation for Ultrasound in Medicine & Biology.

**Key Words:** Stress relaxation, Viscoelasticity, Kelvin-Voigt fractional derivative model, Young's modulus, Prostate, Cancer, Crawling wave sonoelastography.

### INTRODUCTION

Prostate cancer is one of the most common cancers among American men, frequently found by palpation of a firm nodule on digital rectal examination (DRE) or by a blood test of prostate-specific antigen (PSA) level. Currently, transrectal ultrasound (TRUS)-guided biopsy is the only standard for prostate cancer diagnosis. However, this invasive sampling procedure still fails to detect 10–30% of prostate cancers. Therefore, elasticity imaging techniques (either ultrasound-based or magnetic resonance-based) are highly desirable to improve prostate cancer detection. These imaging modalities, along with palpation, are based on the empirical knowledge that prostate cancer is usually stiffer than surrounding normal tissue.

As one of the elasticity imaging modalities, sonoelastography has been systematically investigated and its potential to differentiate between normal and cancerous tissue in human prostate has been demonstrated in a previous article (Taylor et al. 2005). Sonoelastography measures and images the peak displacement of a local particle by analyzing the Doppler variance from the ultrasound echoes. In sonoelastographic images, the brightness of the green channel represents the amplitude of vibration of the local tissue. A stiff lesion is shown as dark green and surrounding normal tissue appears bright green. Figure 1 illustrates a B-mode ultrasound image of an excised human prostate, the corresponding sonoelastographic image and the histology photograph. The malignant tumor is more noticeable in the sonoelastogram than in the sonogram. Quantitative characterization of soft tissues is, therefore, of particular importance for determination of the efficacy of sonoelastography and other elasticity imaging modalities for prostate cancer detection.

Address correspondence to: Man Zhang, Ph.D., Department of Biomedical Engineering, Hopeman Building, Room 319, University of Rochester, Rochester, NY 14627. E-mail: [mazhang@seas.rochester.edu](mailto:mazhang@seas.rochester.edu)

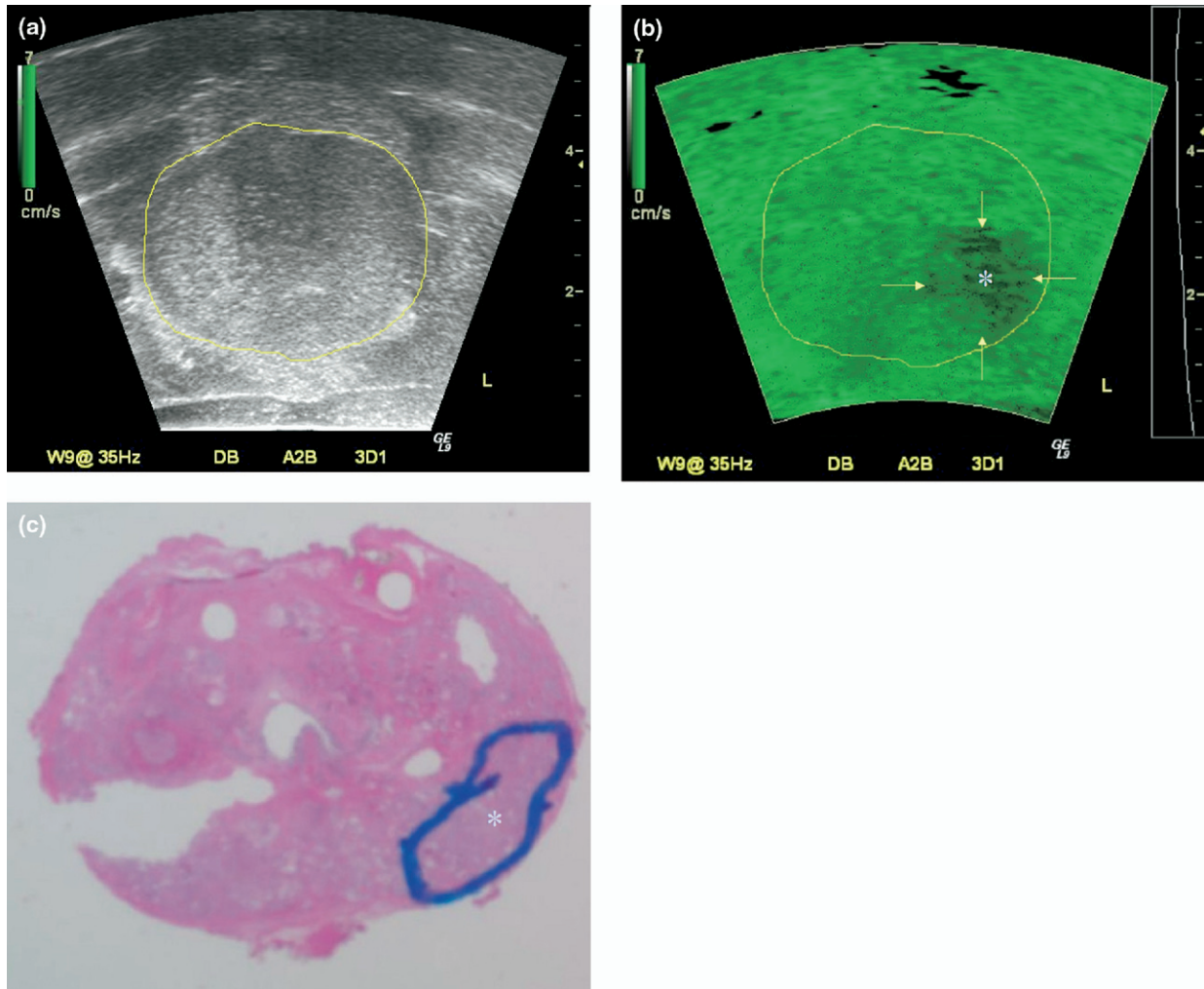


Fig. 1. (a) Matching B-mode ultrasound, (b) sonoelastographic and (c) histologic images of an *in vitro* experiment for prostate cancer detection. The profile of the prostate is delineated in yellow on the B-mode ultrasound image, which is used on the corresponding sonoelastographic image. The sonoelastographic image displays the relative vibration of the tissue. The void in the left posterior region of the mid-gland (marked with arrows and an asterisk) indicates the presence of a stiff mass which is corroborated as a tumor by the histologic image (marked with blue outline and an asterisk). In contrast, the tumor is barely seen on the B-mode image.

Although mechanical properties of structural materials have been studied and well characterized by various mechanical testing methods for decades, the reliable data on soft tissue properties are limited. Several groups (Dunn and Silver 1983; Hof 2003; Huang et al. 2005; Klein et al. 2005; Kuo et al. 2001; Lally et al. 2004; Provenzano et al. 2002; Silver et al. 2001; Suki et al. 1994; Wu et al. 2003) have reported findings on mechanical properties of some soft tissues, but most of their studies were focused on tendons, ligaments, cartilage, skin, muscles, lungs or arteries. In contrast, just a few publications (Jalkanen et al. 2006a, 2006b; Krouskop et al. 1998; Phipps et al. 2005a, 2005b; Yang et al. 2006) presented quantitative results on prostate tissue stiffness. Krouskop et al. (1998) investigated the mechanical properties of normal and diseased prostate tis-

ues with displacement loading experiments. These results showed cancerous tissue had a measurable elevated Young's modulus compared with normal tissue in the same gland. Jalkanen et al. (2006b) measured the stiffness of prostate tissues with a piezoelectric resonance sensor. Subsequently, they related their measurements to tissue morphology and concluded that cancer greatly increases the measured stiffness (Jalkanen et al. 2006a). A British group (Phipps et al. 2005a, 2005b; Yang et al. 2006) also correlated prostate tissue stiffness, tested by dynamic indentation technique, with tissue composition such as the percentage of prostate smooth muscle, epithelium and stroma.

In reality, many soft tissues exhibit both elastic and viscous behavior termed "viscoelastic properties" under biomechanical characterization (Fung 1993). Hence, the

stiffness of tissue has a frequency-dependent response to mechanical vibrations, presented as the viscoelastic modulus. The viscoelastic properties of soft tissues are generally modeled as a combination of springs and dashpots. The choice of tissue model seems to vary with different groups. Besides the three basic linear viscoelastic models (the Maxwell model, the Kelvin-Voigt model and the standard linear solid model) described by Fung (1993), other linear, quasi-linear or nonlinear models have also been applied to describe mechanical testing data. Caputo (1967) first introduced fractional calculus into the field of viscoelasticity. He proposed a modified Kelvin-Voigt (KV) model that consists of a spring in parallel with a dashpot where the stress in the dashpot is equal to the fractional derivative of order  $\alpha$  of the strain. Koeller (1984) derived the stress relaxation function, with a time dependence  $t^{-\alpha}$  in the function for the Kelvin-Voigt fractional derivative (KVFD) model. Later, Bagley and Torvik (1986) described molecular theories that predicted the macroscopic behavior of some viscoelastic polymers and established a link between those theories and the empirical approach from fractional derivative models. Suki *et al.* (1994) argued that the molecular theories derived for polymers may also apply to soft tissues because biological tissues consist of long flexible biopolymers. They used the fractional calculus in biomechanics and discussed the utility of the single fractional dashpot to the KV model. A paper by Szabo and Wu (2000) described a frequency-dependent power law for ultrasound attenuation in soft tissues, suggesting that many soft tissues can be modeled by a generalized KV model, where the dashpot is replaced by a convolution operator. Taylor *et al.* (2002b) further investigated the KVFD model by fitting the liver relaxation data to this model. Dynamic testing was performed by Kiss *et al.* (2004) on canine liver, and the data were fitted to both the KVFD model and the KV model. After comparison of the curve fitting results of the two models, they concluded that the KVFD model had better agreement with the experimental data than the KV model.

Dynamic testing or cyclic loading, however, is dependent on the system. At higher frequencies (*e.g.*, >200 Hz), electronic artifacts dominate. Hence, the results are unlikely precise. Sonoelastography and other studies require understanding of tissue responses at a higher frequency range which cyclic loading cannot provide. The stress relaxation testing combined with the KVFD model may easily address this problem by fitting the relaxation data into the model. Therefore, we propose to use this method to investigate prostate tissue properties at difference frequencies.

This study is our first attempt to use the tissue stress relaxation experiment and the viscoelastic KVFD model for the investigation of the viscoelastic properties of

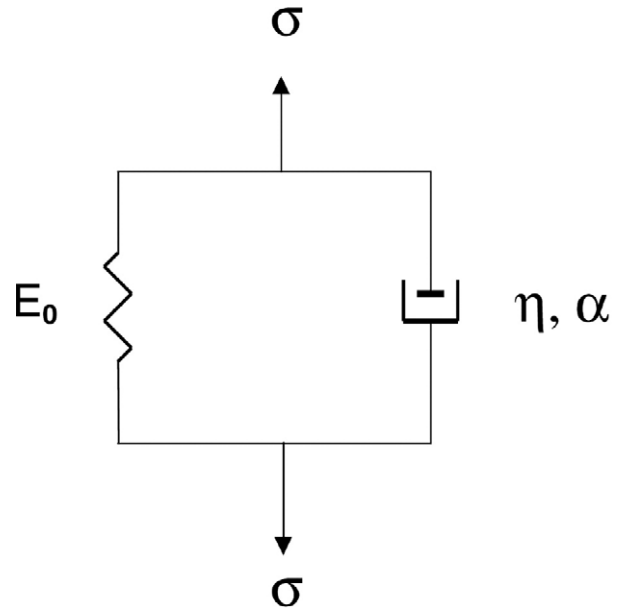


Fig. 2. A diagram of the KVFD model.

human prostate tissues. Results from crawling wave estimation, an independent imaging method, are provided as a comparison. The objectives of this study are two-fold: (i) to establish a reliable and accurate technique for measuring the biomechanical properties of soft tissues, and (ii) to quantitatively characterize and compare the viscoelastic properties of normal and cancerous human prostate tissues *in vitro*.

## MATERIALS AND METHODS

### The Kelvin-Voigt Fractional Derivative (KVFD) model

The KVFD model is a generalization of the KV model. In the KV model, stress in the dashpot is equal to the first derivative with respect to time of the strain. The KVFD model consists of a Hookean spring in parallel with a fractional derivative dashpot (Fig. 2). The stress in the dashpot is equal to the fractional derivative of the strain. The KVFD model contains three parameters:  $E_0$ ,  $\eta$ , and  $\alpha$ , where  $E_0$  refers to the relaxed elastic constant,  $\eta$  refers to the viscoelastic parameter, and  $\alpha$  is the order of fractional derivative. The relationship between stress and strain in the KVFD model is given by the following constitutive differential equation:

$$\sigma(t) = E_0 \varepsilon(t) + \eta D^\alpha [\varepsilon(t)] \quad (1)$$

where  $\sigma$  is stress,  $\varepsilon$  is strain.

$D^\alpha [ ]$  is the fractional derivative operator defined by

$$D^\alpha [x(t)] = \frac{1}{\Gamma(1-\alpha)} \int_0^t \frac{x'(\tau)}{(t-\tau)^\alpha} d\tau \quad (2)$$

where  $\Gamma$  is the gamma function and  $x'(t)$  refers to the first

derivative of the function  $x(t)$  with respect to  $t$ . For the KVFD model we restrict that  $0 < \alpha < 1$ .

#### Stress relaxation

Stress relaxation is one of the characteristics of tissue viscoelasticity. When a viscoelastic material is held at constant strain, the stress decreases with time. To develop a form of the relaxation function, the applied strain is modeled as a ramp of duration  $T_0$ , followed by a hold period of constant strain  $\varepsilon_0$  (Taylor 2002a). So the strain function is:

$$\varepsilon(t) = \begin{cases} (t/T_0)\varepsilon_0 & \text{if } 0 < t < T_0 \\ \varepsilon_0 & \text{when } t \geq T_0 \end{cases} \quad (3)$$

By taking the Laplace transform of the constitutive eqn (1) and eqn (3), we get

$$\sigma(s) = E_0\varepsilon(s) + \eta s^\alpha \varepsilon(s) \quad (4)$$

$$\varepsilon(s) = \frac{\varepsilon_0}{s^2 T_0} (1 - e^{-sT_0}) \quad (5)$$

where  $s$  is the Laplace domain variable. We substitute eqn (4) into eqn (5) and obtain

$$\sigma(s) = E_0 \frac{\varepsilon_0}{s^2 T_0} (1 - e^{-sT_0}) + \eta \frac{\varepsilon_0}{s^{2-\alpha} T_0} (1 - e^{-sT_0}) \quad (6)$$

Then, inverse Laplace transform is applied to both of the terms in eqn (6)

$$\begin{aligned} \sigma(t) = & E_0 \frac{\varepsilon_0}{T_0} (tu(t) - (t - T_0)u(t - T_0)) \\ & + \eta \frac{\varepsilon_0}{\Gamma(2 - \alpha) T_0} (t^{1-\alpha} u(t) - (t - T_0)^{1-\alpha} u(t - T_0)) \end{aligned} \quad (7)$$

where  $u(\cdot)$  is the unit step function. Therefore, during the hold period ( $t \geq T_0$ ) of the stress relaxation curve, the response of a material exhibiting KVFD behavior is

$$\sigma(t) = E_0 \varepsilon_0 + \eta \frac{\varepsilon_0}{\Gamma(2 - \alpha) T_0} (t^{1-\alpha} - (t - T_0)^{1-\alpha}) \quad (8)$$

#### Frequency response: The complex Young's modulus

Frequency-domain response can be obtained from the time-domain response and has a frequency-dependent complex-valued Young's modulus. Taking the Fourier transform of the constitutive eqn (1) yields

$$\sigma(\omega) = E_0 \varepsilon(\omega) + \eta (j\omega)^\alpha \varepsilon(\omega) \quad (9)$$

where  $\omega$  is radian frequency and  $j = \sqrt{-1}$ . The radian frequency is restricted to be positive, *i.e.*,  $\omega \geq 0$ . Because  $\omega = 2\pi f$ , the complex modulus as a function of frequency  $E^*(f)$  is then obtained by

$$\begin{aligned} E^*(f) = \frac{\sigma(f)}{\varepsilon(f)} = & \left[ E_0 + \eta \cos\left(\frac{\pi\alpha}{2}\right) (2\pi f)^a \right] \\ & + j \left[ \eta \sin\left(\frac{\pi\alpha}{2}\right) (2\pi f)^a \right] \end{aligned} \quad (10)$$

The magnitude of  $E^*(f)$  can be expressed as

$$|E^*(f)| = \sqrt{E_0^2 + 2E_0\eta \cos\left(\frac{\pi\alpha}{2}\right) (2\pi f)^a + \eta^2 (2\pi f)^{2a}} \quad (11)$$

From eqn (10) we get the storage modulus,  $E'(f)$ , which is the real part of the complex modulus, and the loss modulus,  $E''(f)$ , which is the imaginary part.

$$E'(f) = E_0 + \eta \cos\left(\frac{\pi\alpha}{2}\right) (2\pi f)^a \quad (12)$$

$$E''(f) = \eta \sin\left(\frac{\pi\alpha}{2}\right) (2\pi f)^a \quad (13)$$

The storage modulus is related to the elasticity of the soft tissue, whereas the loss modulus is related to the viscosity.

#### Prostate specimen preparation

Human prostates were obtained from the Pathology Department at the University of Rochester Medical Center immediately after radical prostatectomy. The experimental protocol was approved by our institutional review board, and written informed consents to have mechanical testing performed were obtained from prostate cancer patients before radical prostatectomy. The prostate was sectioned. Then cylindrical cores (approximately 8 mm in diameter and 7 mm in length) were acquired from the posterior zone of the prostates where cancer often occurs (Cheng et al. 2005). A total of 17 fresh tissue specimens were collected from eight patients who had not received any hormone treatment before surgery. The mean age of the patients was 63 y (range 55–76) and the mean PSA level was 6.1  $\mu\text{g/mL}$  (range 3.6–9). The prostate specimens had a Gleason score of 3 + 4 or greater, according to the reports from the Pathology Department. The core samples were soaked in saline before mechanical testing. Within 2 h of prostate resection, mechanical testing was performed on the tissue samples at room temperature. We assumed the prepared tissue specimens are isotropic and homogeneous.

#### Mechanical testing and curve fitting

A 1/S mechanical device (MTS Systems Co., Eden Prairie, MN, USA) with a 5 Newton load cell was used to test the core samples (Fig. 3). The upper and lower platens were coated with vegetable oil before testing. To



Fig. 3. Experimental set-up for mechanical testing of prostate core samples.

minimize the dehydration effect, the side of each sample was coated with a thin layer of petroleum jelly. The core sample was then put on the center of the lower testing plate. The top plate was used as a compressor and carefully positioned to fully contact the sample. After two minutes for tissue recovery from precompression, a uniaxial unconfined compression controlled by TestWorks 3.10 software (Software Research, Inc., San Francisco, CA, USA) was conducted to measure the time-domain stress relaxation data at room temperature. The compression rate and the strain value were adjusted to 0.5 mm/s and 5%, respectively. Throughout the test the stress required to maintain the specified compression was recorded. Tests lasted about 700 s. The resulting data consists of a plot of the stress *vs.* time under 5% strain. Multiple measurements were performed on each sample sequentially with 15-min intervals in between. Samples were put back in saline during intervals to prevent dehydration. The stress-relaxation curve of each sample during the hold period was fit to the KVFD model using the MATLAB Curve Fitting Toolbox (The MathWorks, Inc., Natick, MA, USA). Nonlinear least squares fitting was applied on each curve. The averaged three model parameters,  $E_0$ ,  $\eta$  and  $\alpha$ , were then obtained. These model parameters were then used in eqn (10) to predict the value of the complex modulus at any frequency using the KVFD model.

#### *Histologic assessment*

After mechanical testing, prostate core samples were fixed in 10% formalin solution for at least 24 h, and then sent to the Pathology Department. Routine histology with hematoxylin and eosin (Richard-Allan Scientific, Kalamazoo, MI, USA) staining was performed by histopathology technicians. At least two histologic slices were

obtained from each core. The slices were analyzed by pathologists using microscopy. Then the cancer percentage was measured and reported for the investigation of the correlation between mechanical and histologic findings. The pathologists were blinded to the results of mechanical testing. Prostate specimens containing more than 50% cancer were considered cancerous tissue. The range of cancer in these specimens was from 60% (one sample) to 100% (three samples), with an average of 83%. The normal specimens were cancer free and did not have obvious BPH, inflammation or calcification. Note that tissue samples containing <50% cancer were excluded in this study.

#### *Statistical analysis*

The averaged magnitudes of complex Young's moduli of cancer and normal tissue are expressed as mean  $\pm$  standard deviation in kPa, which gives an elastic contrast between the two types of tissues. Two-sample *t*-test was used to assess the differences between the mechanical properties of normal and cancerous tissues in the same prostate. Statistical significance ( $p < 0.01$ ) was provided for the viscoelastic parameter  $\eta$  and the magnitude of complex Young's modulus  $|E^*|$ .

#### *Crawling wave estimation*

Crawling wave sonoelastography, an ultrasound-based approach conducted in our laboratory, was utilized to characterize the mechanical properties of human prostate as well. In this experiment, crawling waves (or slowly moving shear wave interference patterns) were generated using a pair of mechanical sources (vibrating at slightly offset frequencies, *e.g.*, 150 and 150.15 Hz) positioned on opposing sides of the gelatin embedded prostate gland (Wu *et al.* 2004). Imaging was performed using a GE Logiq 9 ultrasound scanner (GE Ultrasound, Wauwatosa, WI, USA) modified for sonoelastography, with raw data saved for processing. Shear velocity sonoelastograms were produced off-line from the reconstructed crawling wave images using a 2-D autocorrelation-based estimation technique (Hoyt *et al.* 2007). The Young's modulus can be obtained from the estimated shear wave velocity.

## RESULTS

Figure 4a shows stress relaxation curves of cancerous and normal specimens obtained from the same prostate at 5% strain. Each curve fitting had a correlation coefficient ( $r^2$ ) value larger than 0.98, demonstrating that the stress relaxation curves were fit very well to the KVFD model. The frequency-dependent Young's moduli of the cancerous and normal tissues were then calculated from the model, and the results are illustrated in

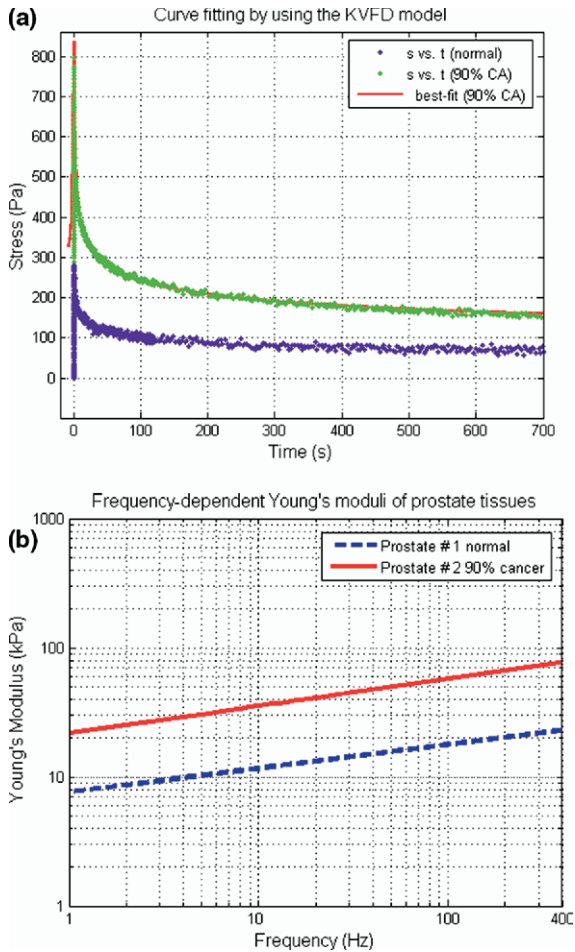


Fig. 4. (a) Stress relaxation curves of a cancerous specimen and a normal specimen obtained from the same prostate at 5% strain. (b) The Young's moduli of the two types of prostate tissues are plotted against frequency, showing a positive relation between tissue stiffness and cancer percentage. It is noted that the frequency-dependent modulus curves are averaged from three repetitive tests. The errors were <5%.

Fig. 4b. In this case, the magnitudes of complex Young's moduli are 62.9 kPa and 19.2 kPa at 150 Hz. The elastic contrast is about 3.3:1 at 150 Hz.

Table 1 summarizes the best-fit parameters and  $r^2$  values for all of the examined samples. The complex Young's modulus in the frequency-domain was determined with those model parameters. However,  $E_0$  was not included in the table because curve fitting results

gave the examined soft tissues values of  $E_0$  approaching zero. To extract the relaxed spring parameter  $E_0$ , we note that in eqn (8),  $\sigma(\infty) = E_0 \epsilon_0$ , meaning when equilibrium is reached,  $E_0$  is the value of stress  $\sigma$  divided by the applied strain,  $\epsilon_0$ . As we know, the stress of a perfectly elastic material would be constant with time, whereas for a Newtonian fluid, the stress level would relax rapidly to zero. In our stress relaxation tests, the stress response did not reach the equilibrium status for a long time and the stress level was approaching zero asymptotically, indicating the tested soft tissues are viscoelastic materials with long time-constant fluidlike behavior. To further confirm this phenomenon, several long span tests were performed on human prostate tissues. The testing method and conditions were the same as those described in *Materials and Methods*, except the relaxation time was much longer (>2,000 s). Although we could not record the stress relaxation curves longer to reach the plateau because of the limit of the mechanical testing system, we did observe a trend that the stress levels approached zero, except one sample containing 100% cancer, which showed  $E_0 = 746$  Pa, a small, non-negligible value. This finding indicates that the parameter  $E_0$  in the KVFD model had a relatively small value and did not contribute significantly to the overall elasticity in our tests. However, for other soft tissues,  $E_0$  may not always be negligible.

The viscoelastic stress relaxation behaviors of the examined prostate tissues were well characterized by the KVFD model, with  $r^2$  larger than 0.97. The magnitudes of complex Young's moduli of prostate tissues are averaged and plotted as a function of frequency in Fig. 5. The frequency ranges from 25 to 300 Hz as the vibration frequency of sonoelastography is generally set in this range. The error bars represent the standard deviation of the experimental data. The variation of multiple measurements for each sample was <10%. Although the frequency dependence of the Young's moduli was not measured directly in this study, the KVFD model predicts that prostate tissues have the Young's moduli that slightly increase with frequency in the range for sonoelastography imaging (Fig. 5).

The average magnitudes of the complex Young's moduli of cancerous and normal tissues are  $40.4 \pm 15.7$  kPa and  $15.9 \pm 5.9$  kPa at 150 Hz, respectively, giving an elastic contrast of  $(2.6 \pm 0.9):1$ . Using eqns (12) and

Table 1. Best-fit parameters and  $r^2$  values for all examined samples

Prostate tissue	No. of samples	$\eta$ (kPa s <sup><math>\alpha</math></sup> )	$\alpha$	$r^2$	$ E^* @150\text{Hz}$ (kPa)
Normal	8	$3.61 \pm 1.25$	$0.2154 \pm 0.0417$	0.9740	$15.9 \pm 5.9$
Cancer >50%	9	$8.65 \pm 3.40$	$0.2247 \pm 0.0304$	0.9921	$40.4 \pm 15.7$

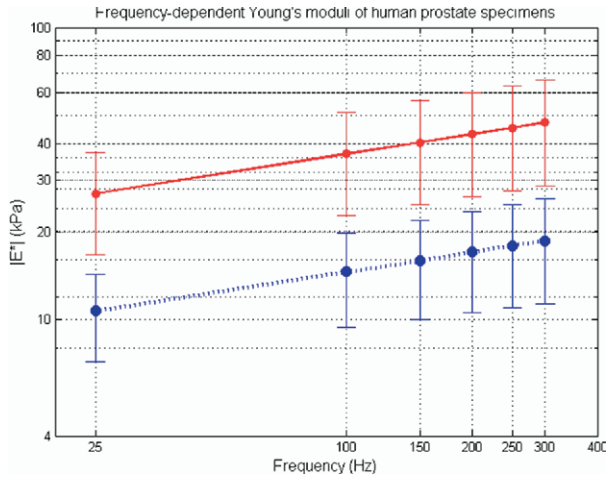


Fig. 5. Plot of averaged magnitudes of complex Young's moduli of normal (blue dotted curve) and cancerous (red solid curve) prostate tissues as a function of frequency. Standard deviations were also provided.

(13), the storage modulus was calculated as greater than the loss modulus by a factor of  $2.8 \pm 0.3$  for the normal tissue and a factor of  $2.7 \pm 0.3$  for the cancer in the tested frequency range. This means that the elasticity-to-viscosity ratios of the normal prostate tissue and the cancerous tissue are  $2.8 \pm 0.3:1$  and  $2.7 \pm 0.3:1$ , respectively. For both normal ( $n = 8$ ) and cancerous ( $n = 9$ ) prostate specimens, there are noticeable inter-patient variabilities in the mechanical properties. Nine two-sample *t*-tests (one normal/cancer pair per prostate except one prostate that had two paired samples) indicated there were significant differences between mechanical properties of the cancer and normal tissue in the same gland:  $\eta$  ( $p < 0.01$ ) and  $|E^*|$  ( $p < 0.01$ ).

Pathologists noted that it was difficult to distinguish cancer from noncancer by direct eye observation of the cores. As mentioned earlier, pathologic specimens containing 50% or more cancer were under investigation. The histologic findings indicate that the prostate cancer is entirely made up of malignant prostate glands or epithelial tissue (ET). A core specimen with 70% cancer means that there are 70% malignant prostate glands or ET and 30% stroma. Figure 6 shows the histology of a normal core sample and core samples containing 70% and 100% cancer. In Fig. 7, there is a noticeable clustering of the cancerous prostate data disjoint from the normal stiffness values.

Figure 8 shows that crawling waves propagate through an *in-vitro* prostate containing a malignant tumor. The stiffness values were 65.6 and 19.8 kPa for the cancer and normal tissue, respectively. Hence, the elastic contrast was about 3.3:1. This data are in good agreement with our mechanical testing results.

## DISCUSSION

Previous studies have revealed that most biological soft tissues exhibit viscous behavior in addition to their better-known elastic properties. The KVFD model is a three-parameter spring and dashpot model that uses fractional calculus to characterize soft tissue viscoelasticity. The KV model is actually a particular form of the KVFD model. In other words, we can get the KV model by setting parameter  $\alpha$  to be 1 in the KVFD model. In this paper, we presented the utility of the KVFD model for modeling the stress relaxation responses of normal and cancerous prostate tissues. The prostate stress relaxation data were also fit to the KV model for comparison. The  $r^2$  values were  $< 0.4$ .

The fractional derivative dashpot in the KVFD model consists of not only the viscous component but also the elastic component, with the modulus having both real and imaginary components. Even when  $E_0$  is very small, the storage modulus, corresponding to the elastic behavior of the tested soft tissue, is still greater than the loss modulus, the viscous response of the tissue, by a factor of 2.7 or more. The value of  $\alpha$  is noticeably related to the viscosity of the material because the loss modulus increases in accord with  $\alpha$ . The same tendency was found in the slope of the Young's modulus vs. frequency curve, which increases with rising  $\alpha$ .

To reduce the variability of measurements on each sample, it is essential to section the upper and lower surfaces of the cylindrical sample as parallel and as flat as possible for compression tests. However, this requirement is hard to achieve, especially when the sample is very soft, such as fresh liver and prostate. Two blades in parallel were used for sample sectioning. Multiple tests were conducted on each sample, and the results were averaged. Our results indicated that the variability because of imperfect shape of the sample was relatively small, as we expected.

During mechanical testing, we did not observe any loss of contact between the tested sample and the compressor that would result in a loss of surface tension and produce a discontinuity in the data, which was not present. In fact, the stress levels only approached zero smoothly and asymptotically, in a way that fit well with the KVFD model with a small value of  $E_0$ . Moreover, the applied force of the upper platen was greater than 0.02 N, whereas the force of gravity on the samples was in the range of 0.003 to 0.004 N, which is much smaller. If the gravitational loading is considered, the resulting difference of the complex Young's modulus is  $< 5\%$ . Therefore, we believe that the gravitational loading of each core sample is negligible.

The histologic findings reveal that overall the cancerous samples exhibit increased stiffness compared with

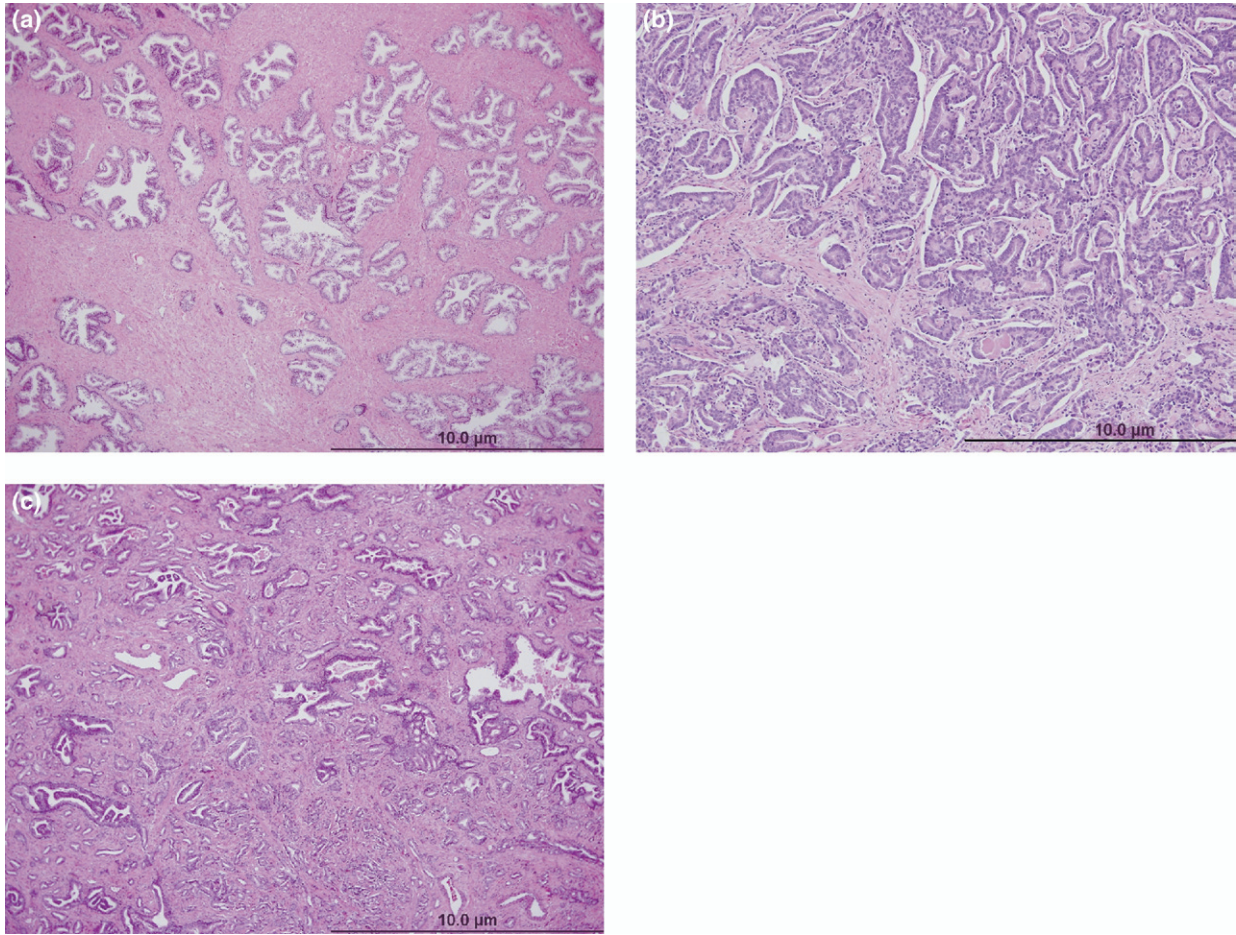


Fig. 6. Histology photographs of (a) a normal core sample and core samples containing (b) 70% cancer and (c) 100% cancer.

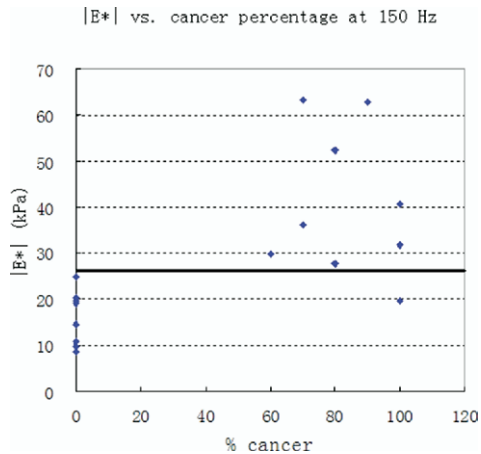


Fig. 7. Tissue stiffness (the Young’s modulus) vs. cancer percentage in the examined core samples. The black line separates the stiffness values of cancerous tissues and those of the normal tissues.

the normal tissue. The two types of tissues can be separated easily by a black line in Fig. 7. The wide stiffness range relative to the cancer percentage may be related to the following factors: (i) noticeable interpatient variabilities were found in prostate tissue stiffness; (ii) the histologic results were obtained from the analysis of two or three cross-section slices from each core sample, rather than the whole tissue core; and (iii) the imperfect shape of the core samples may be a contributing factor although its effect was minor.

Several elasticity imaging modalities have also been advanced to quantify tissue mechanical properties. Kemper et al. (2004) investigated the stiffness of healthy human prostates with an *in-vivo* magnetic resonance elastography (MRE). Their measurements indicated that the peripheral portion of the prostate was stiffer than the central portion. The mean Young’s modulus values were 9.9 kPa and 6.6 kPa, respectively. Our results on normal prostate tissue characterization are comparable with the data reported by Kemper et al. (2004). Good agreement

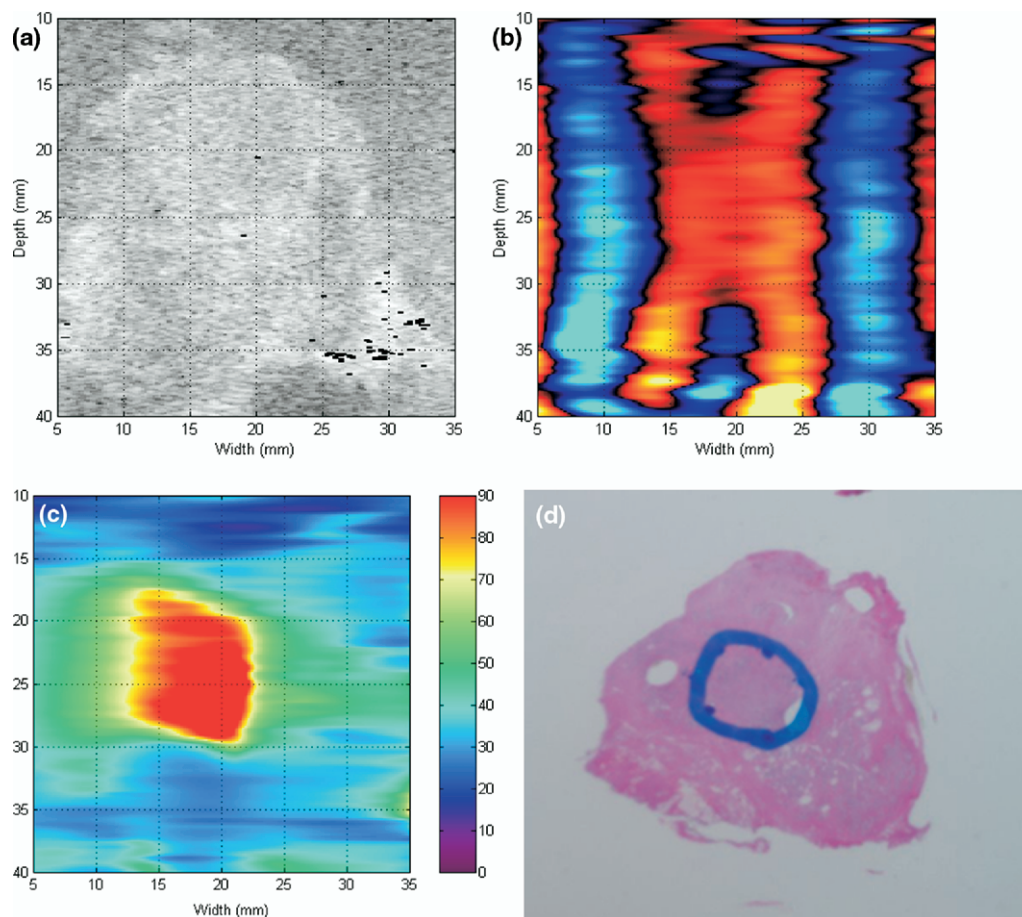


Fig. 8. Experimental sonoelastographic imaging results depicting matched (a) B-mode ultrasound image, (b) crawling-wave sonoelastogram with measurable interference patterns shown as blue and red fringes, (c) quantitative sonoelastogram and (d) histology photograph in which the blue circle delineates where the cancer is located. The quantitative sonoelastogram is calculated from the crawling-wave sonoelastogram and depicts local Young's moduli distributions in units of kPa.

was also found between the mechanical testing results and the measurements obtained from crawling-wave sonoelastography. The detailed comparison of these two methods for tissue characterization can be found in an earlier paper (Zhang *et al.* 2007). In contrast, Krouskop *et al.* (1998) reported benign prostatic hyperplasia (BPH) had significantly lower values (36–41 kPa) than normal tissue; the normal anterior and posterior tissue had elastic modulus values of 55–71 kPa under 2% or 4% precompression, whereas cancer had values of 96–241 kPa. Furthermore, Phipps *et al.* (2005b) reported a wide range, from 40–140 kPa, of the elastic component of normal prostate tissue. The divergence is mainly caused by the different choices of testing techniques; testing conditions such as compression frequencies, temperature and humidity; sample variation; tissue models; and other experimental factors. In particular, the assumption of a particular tissue model, for example, purely elastic *vs.* vis-

coelastic, can greatly influence the estimates of tissue properties.

## CONCLUSIONS

This study systematically investigated viscoelastic properties of normal and cancerous human prostate tissues. The stress relaxation testing and the KVFD modeling approaches provide the frequency-dependent storage and loss moduli, from which both elastic and viscous behavior can be extracted. For *in-vitro* conditions, the elastic contrast between cancer and normal appears to be 2.6:1 at 150 Hz, although the *in-vivo* contrast could be higher as a result of the additional effects of elevated interstitial pressure (Weaver *et al.* 2007).

In summary, this paper achieves two important accomplishments. First, mechanical stress relaxation with results fit to the KVFD model successfully characterized

viscoelastic properties of prostate tissues *in vitro*, offering a simple but effective approach to quantify soft tissue properties. The frequency-dependent nature of the Young's modulus may provide useful information, such as tissue viscosity, to advance tissue characterization. Second, the results quantify the elastic contrast between cancerous and normal prostate tissues, and this contributes to the limited information in the literature on the viscoelastic properties of human prostate.

*Acknowledgements*—We thank Diana Scott for the histology slice preparation, and Larry Taylor, Art Salo and Amy Lerner for their help on the mechanical testing set-up. The authors also thank GE Ultrasound. This study was supported by NIH grant 5 RO1 AG016317–05.

## REFERENCES

- Bagley RL, Torvik PJ. A theoretical basis for the application of fractional calculus to viscoelasticity. *J Rheology* 1986;30:133–155.
- Caputo M. Linear models of dissipation whose  $q$  is almost frequency independent-II. *Geophys J R Astr Soc* 1967;13:529–539.
- Cheng L, Jones TD, Pan CX, Barbarin A, Eble JN, Koch MO. Anatomic distribution and pathologic characterization of small-volume prostate cancer (<0.5 ml) in whole-mount prostatectomy specimens. *Mod Pathol* 2005;18:1022–1026.
- Dunn MG, Silver FH. Viscoelastic behavior of human connective tissues: Relative contribution of viscous and elastic components. *Connect Tissue Res* 1983;12:59–70.
- Fung YC. *Biomechanics: Mechanical Properties of Living Tissues*. New York: Springer-Verlag, 1993.
- Hof AL. Muscle mechanics and neuromuscular control. *J Biomech* 2003;36:1031–1038.
- Hoyt K, Parker KJ, Rubens DJ. Real-time shear velocity imaging using sonoelastographic techniques. *Ultrasound Med Biol* 2007;33:1086–1097.
- Huang CY, Wang VM, Pawluk RJ, Bucchieri JS, Levine WN, Bigliani LU, Mow VC, Flatow EL. Inhomogeneous mechanical behavior of the human supraspinatus tendon under uniaxial loading. *J Orthop Res* 2005;23:924–930.
- Jalkanen V, Andersson BM, Bergh A, Ljungberg B, Lindahl OA. Prostate tissue stiffness as measured with a resonance sensor system: A study on silicone and human prostate tissue *in vitro*. *Med Biol Eng Comput* 2006a;44:593–603.
- Jalkanen V, Andersson BM, Bergh A, Ljungberg B, Lindahl OA. Resonance sensor measurements of stiffness variations in prostate tissue *in vitro*—A weighted tissue proportion model. *Physiol Meas* 2006b;27:1373–1386.
- Kiss MZ, Varghese T, Hall TJ. Viscoelastic characterization of *in vitro* canine tissue. *Phys Med Biol* 2004;49:4207–4218.
- Klein TJ, Chaudhry M, Bae WC, Sah RL. Depth-dependent biomechanical and biochemical properties of fetal, newborn, and tissue-engineered articular cartilage. *J Biomech* 2007;40:182–190.
- Koeller RC. Applications of fractional calculus to the theory of viscoelasticity. *J Appl Mech Trans ASME* 1984;51:299–307.
- Krouskop TA, Wheeler TM, Kallel F, Garra BS, Hall T. Elastic moduli of breast and prostate tissues under compression. *Ultrasound Imaging* 1998;20:260–274.
- Kuo PL, Li PC, Li ML. Elastic properties of tendon measured by two different approaches. *Ultrasound Med Biol* 2001;27:1275–1284.
- Lally C, Reid AJ, Prendergast PJ. Elastic behavior of porcine coronary artery tissue under uniaxial and equibiaxial tension. *Ann Biomed Eng* 2004;32:1355–1364.
- Phipps S, Yang TH, Habib FK, Reuben RL, McNeill SA. Measurement of the mechanical characteristics of benign prostatic tissue: A novel method for assessing benign prostatic disease. *Urology* 2005a;65:1024–1028.
- Phipps S, Yang TH, Habib FK, Reuben RL, McNeill SA. Measurement of tissue mechanical characteristics to distinguish between benign and malignant prostatic disease. *Urology* 2005b;66:447–450.
- Provenzano PP, Lakes RS, Corr DT, Vanderby R, Jr. Application of nonlinear viscoelastic models to describe ligament behavior. *Bio-mech Model Mechanobiol* 2002;1:45–57.
- Silver FH, Horvath I, Foran DJ. Viscoelasticity of the vessel wall: The role of collagen and elastic fibers. *Crit Rev Biomed Eng* 2001;29:279–301.
- Suki B, Barabasi AL, Lutchen KR. Lung tissue viscoelasticity: A mathematical framework and its molecular basis. *J Appl Physiol* 1994;76:2749–2759.
- Szabo TL, Wu J. A model for longitudinal and shear wave propagation in viscoelastic media. *J Acoust Soc Am* 2000;107:2437–2446.
- Taylor LS. Three-dimensional sonoelastography: Principles and practices with applications to tumor visualization and volume estimation. Ph.D. dissertation, University of Rochester 2002a.
- Taylor LS, Lerner AL, Rubens DJ, Parker KJ. A Kelvin-Voigt fractional derivative model for viscoelastic characterization of liver tissue. ASME International Mechanical Engineering Congress and Exposition, New Orleans, Louisiana, 2002b.
- Taylor LS, Rubens DJ, Porter BC, Wu Z, Baggs RB, di Sant'Agnese PA, Nadasdy G, Pasternack D, Messing EM, Nigwekar P, Parker KJ. Prostate cancer: Three-dimensional sonoelastography for *in vitro* detection. *Radiology* 2005;237:981–985.
- Weaver JB, Perrinez PR, Bergeron JA, Kennedy FE, Wang H, Scott Lollis S, Doyley MM, Hoopes PJ, Paulsen KD. The effects of interstitial tissue pressure on the measured shear modulus *in vivo*. *Proc SPIE* 2007;6511:65111A–65111.
- Wu JZ, Dong RG, Smutz WP, Schopper AW. Nonlinear and viscoelastic characteristics of skin under compression: Experiment and analysis. *Biomed Mater Eng* 2003;13:373–385.
- Wu Z, Taylor LS, Rubens DJ, Parker KJ. Sonoelastographic imaging of interference patterns for estimation of the shear velocity of homogeneous biomaterials. *Phys Med Biol* 2004;49:911–922.
- Yang TH, Leung SK, Phipps S, Reuben RL, McNeill SA, Habib FK, Schieder A, Stevens R. *In-vitro* dynamic micro-probing and the mechanical properties of human prostate tissues. *Technol Health Care* 2006;14:281–296.
- Zhang M, Castaneda B, Wu Z, Nigwekar P, Joseph JV, Rubens DJ, Parker KJ. Congruence of imaging estimators and mechanical measurements of viscoelastic properties of soft tissues. *Ultrasound Med Biol* 2007;33:1617–1631.